



Expanding TRANS4D's Scope to Include 3D Crustal Velocity Estimates for a Neighborhood of the Caribbean Plate

Richard Snay, Ph.D.¹; Jarir Saleh²; Michael Dennis, Ph.D., P.E., M.ASCE³;
Charles DeMets, Ph.D.⁴; and Héctor Mora-Páez, Ph.D.⁵

Abstract: This paper introduces Version 0.3 of the TRANS4D software, where TRANS4D is short for Transformations in Four Dimensions. TRANS4D enables geospatial professionals and others to transform three-dimensional (3D) positional coordinates across time and among several popular terrestrial reference frames. Version 0.3 includes a crustal velocity model for a neighborhood of the Caribbean plate in the form of 3D crustal velocity estimates at the nodes of a two-dimensional grid in latitude and longitude. This velocity model supplements existing TRANS4D velocity models for the continental United States and for parts of Alaska and Canada. This paper also introduces a terrestrial reference frame, called the Caribbean Terrestrial Reference Frame of 2014 (CATRF2014), which was derived from horizontal crustal velocities for 25 geodetic stations. These stations are considered to be “stable” relative to one another, because each has a horizontal velocity whose magnitude is less than 1.0 mm/year relative to CATRF2014. This new reference frame is defined in terms of a three-parameter transformation from the International Global Navigation Satellite System Service 2014 (IGS14) reference frame, which can be considered identical to the International Terrestrial Reference Frame of 2014 (ITRF2014). These three parameters correspond to the Euler-pole parameters that hopefully quantify the motion of the stable interior of the Caribbean plate. However, the location of this stable interior is not well known because most of it resides underwater. DOI: [10.1061/\(ASCE\)SU.1943-5428.0000377](https://doi.org/10.1061/(ASCE)SU.1943-5428.0000377). © 2021 American Society of Civil Engineers.

Introduction

Snay et al. (2016) introduced numerical models that quantify three-dimensional (3D) crustal velocities as a function of latitude and longitude for the conterminous United States (CONUS) and for most of Alaska and Canada. These models provide the foundation for Version 0.1 of the TRANS4D software, where TRANS4D is short for Transformations in Four Dimensions. TRANS4D is being developed to enable geospatial professionals and others to apply estimated velocities when transforming 3D positional coordinates referred to one date to corresponding 3D positional coordinates referred to an alternative date. Moreover, users can apply TRANS4D to transform positional coordinates from one terrestrial reference frame to another for a suite of popular reference frames, including all existing realizations of the International Terrestrial Reference System, plus all existing reference frames of the International Global Navigation

Satellite System Service (IGS) and the World Geodetic System 1984, as well as three regional frames of the North American Datum of 1983 (referenced to the North America, Pacific, and Mariana tectonic plates, respectively). TRANS4D also addresses changes in positional coordinates due to phenomena other than constant velocities. In particular, TRANS4D contains models quantifying the coseismic displacements associated with 31 North American earthquakes, and a model for the postseismic motion associated with the M7.9 Denali Fault earthquake that occurred in central Alaska on November 3, 2002. This paper, however, will address only the particular crustal motion associated with constant velocities.

TRANS4D's velocity models include a collection of two-dimensional (2D) grids (in latitude and longitude) where each grid spans a specified spherical rectangle, and where an estimated 3D velocity (north, east, up components) is recorded for each grid node, together with the three standard deviations associated with these three velocity components. For each point located within the span of a given rectangular grid, TRANS4D employs bilinear interpolation to estimate the point's 3D velocity and its associated three standard deviations from the corresponding values stored at the four nodes that define the grid cell encompassing the location of interest.

The velocity models encoded in TRANS4D have been derived from repeated geodetic observations—primarily GNSS observations—but leveling, trilateration, and other geodetic data types have also been employed. Thanks to the rapid increase in the number of continuously operating GNSS stations distributed around the world, velocity models can be upgraded relatively frequently. Accordingly, Version 0.2 of TRANS4D was recently released (Snay et al. 2018). Version 0.2 provides a much-improved velocity model for that part of CONUS located west of longitude 107° W. The more accurate velocities residing in Version 0.2 benefited from the use of an improved velocity-interpolation algorithm

¹Retired, 427 Homewood Circle, Frederick, MD 21702; formerly, Geodesist, NOAA's National Geodetic Survey, 1315 East-West Highway, Silver Spring, MD 20190 (corresponding author). ORCID: <https://orcid.org/0000-0002-5942-1577>. Email: rssnay@aol.com

²Geodesist, NOAA's National Geodetic Survey, 1315 East-West Highway, Silver Spring, MD 20190.

³Geodesist, NOAA's National Geodetic Survey, 1315 East-West Highway, Silver Spring, MD 20190. ORCID: <https://orcid.org/0000-0002-9286-7407>

⁴Professor, Dept. of Geoscience, Univ. of Wisconsin, A350 Weeks Hall, Madison, WI 53706.

⁵Coordinator, Geological Survey of Colombia, Space Geodesy Research Group, Diagonal 53 No. 34-53, Bogotá 111321, Colombia.

Note. This manuscript was submitted on March 26, 2021; approved on July 1, 2021; published online on September 15, 2021. Discussion period open until February 15, 2022; separate discussions must be submitted for individual papers. This paper is part of the *Journal of Surveying Engineering*, © ASCE, ISSN 0733-9453.

compared to that used for the original TRANS4D version, as well as longer observational histories at many of the stations involved in Version 0.1. Also, Version 0.2 benefitted from the existence of estimated velocities at many additional geodetic stations.

In this paper, Version 0.3 of TRANS4D is introduced. This new version includes a 3D velocity model for a spherical rectangle encompassing a neighborhood of the Caribbean plate. This rectangle ranges between latitudes 6° N and 24° N and between longitudes 57° W and 95° W. Its associated velocity grid has a mesh of 0.0625° by 0.0625°. Fig. 1 displays the area spanned by this grid together with geodetic stations involved in estimating a 3D velocity at each node of this grid. Moreover, Fig. 1 identifies seven tectonic plates and/or microplates that collectively span this spherical rectangle. The plate boundaries presented in Fig. 1 reflect those provided by the digital model published by Bird (2003).

This paper also introduces estimates for the three parameters that quantify the Euler pole and the rotation rate about this pole, which may be applied to define a transformation from the International GNSS Service 2014 (IGS14) reference frame (Rebischung et al. 2016) to a new terrestrial reference frame in which the transformed horizontal velocities of 25 existing geodetic stations each has a magnitude of less than 1.0 mm/year. Hence, these 25 stations are considered to be rigid relative to one another. This new terrestrial reference frame is herein referred to as CATRF2014, as it constitutes a preliminary realization of the Caribbean Terrestrial Reference Frame of 2022 (CATRF2022) to be developed by the National Geodetic Survey (NGS)—an office of the National Oceanic and Atmospheric Administration (NOAA)—in or around the 2025 timeframe (NGS 2020). Note that NGS does not recognize CATRF2014 as an official reference frame for general use. CATRF2014 was developed only for research and instructional purposes.

Because the CATRF2014 realization was derived using GNSS data referred to IGS14, it is formally defined with respect to the

IGS14 reference frame. IGS14 is a GNSS-only solution aligned with the International Terrestrial Reference Frame of 2014 (ITRF2014) at epoch 2010.00 (Altamimi et al. 2016; Rebischung et al. 2016). Therefore, IGS14 can be considered equivalent to ITRF2014 from a frame definition and transformation perspective (and they are treated as identical within TRANS4D).

Throughout this paper, the vertical velocity at a point refers to the rate of change over time of the ellipsoidal height at this point relative to an ellipsoid whose size and shape equal those adopted for the Geodetic Reference System of 1980 (Moritz 2000).

Geodetic Data

The new 3D velocity model for the Caribbean has been formulated by using velocity vectors derived from geodetic observations. These velocity vectors were obtained from 16 separate data sets provided by multiple institutions and researchers. In many cases, a velocity vector contained in one data set may have been computed from essentially the same geodetic data used to compute a velocity vector contained in another data set. The 16 data sets include the following:

- The IGS data set based on continuous GNSS data observed between January 2, 1994, and December 30, 2018, at more than 1,500 IGS-affiliated stations distributed around the world (NASA/GSFC 2019). The IGS updates its solution on a weekly basis. These velocities are referred to the IGS14 reference frame.
- A data set published by Wang et al. (2019) consisting of 3D velocity vectors derived from Global Positioning System (GPS) data observed between 2012 and 2018 at 250 continuously operating GNSS stations located on or near the Caribbean plate. These velocities are referred to the CARIB18 reference frame whose development is described in that publication.

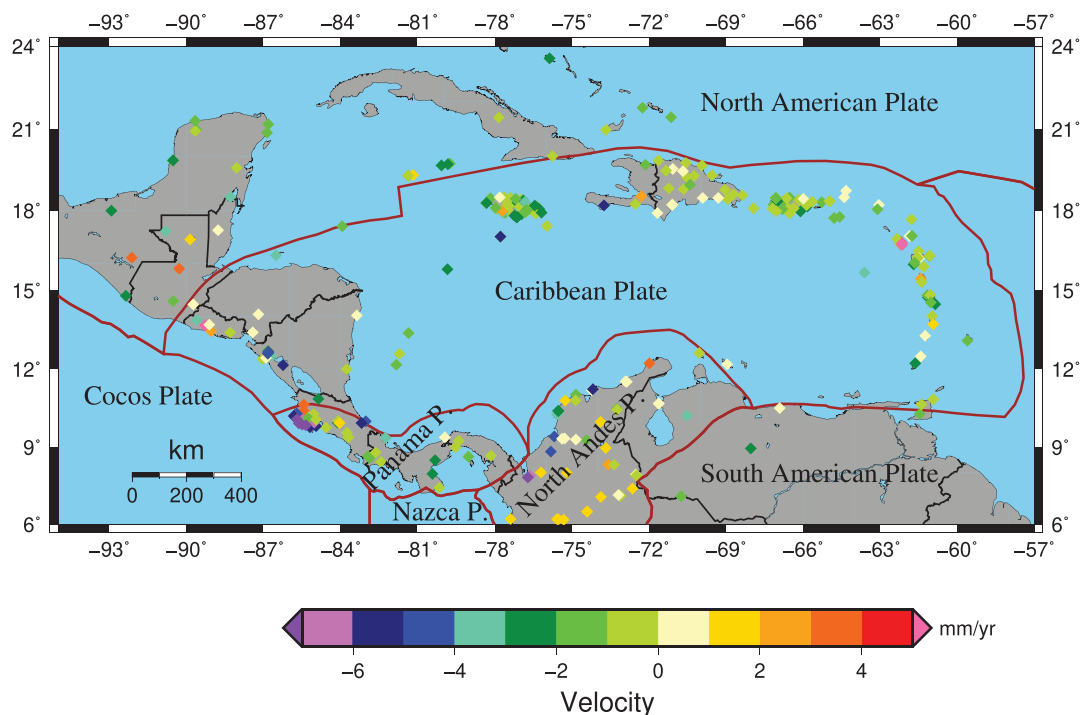


Fig. 1. (Color) Caribbean study area. Colored diamonds identify geodetic stations at which IGS14 vertical velocities have been estimated with standard deviations ≤ 2.0 mm/year. Each diamond's color reflects the station's Stage-2 IGS14 vertical velocity. Brown line segments approximate tectonic plate boundaries. Black line segments denote national borders.

- A data set published by Ellis et al. (2018) composed of IGS08-consistent 2D horizontal velocities derived from GPS data observed (some continuously and others in campaign mode) between 1999 and 2017 at 201 geodetic stations located in northern Central America and southern Mexico. Ellis et al. (2019) discusses the implications of these velocities in great detail.
- An unpublished set of IGS14-consistent 3D velocities provided by Charles DeMets and derived from GNSS data observed between 1998 and 2020 at 50 stations located in the vicinity of Jamaica.
- The 2017 Sistema de Referencia Geocéntrico para las Americas (SIRGAS) solution that provides IGS14-consistent 3D velocities for continuously operating GNSS stations distributed throughout parts of South America and North America. These velocities are based on GNSS data observed between 2011 and 2017, and Sánchez and Drewes (2020) discuss the implications of these velocities in great detail.
- A data set published by Mora-Páez et al. (2019) containing ITRF2008-consistent 2D horizontal velocity vectors derived from GPS data (observed prior to 2016) at 60 continuously operating stations located in northwestern South America and the southwest Caribbean.
- An unpublished set of ITRF2014-consistent 3D velocities for 69 continuously observed GNSS stations located throughout this paper's study area, but with a concentration located in the vicinity of Colombia. These velocities were computed by the Space Geodesy Research Group of the Geohazards Directorate, Geological Survey of Colombia.
- A data set produced by Saleh et al. (2021) that provides IGS14-consistent 3D velocity vectors derived from GPS data observed between 1996 and 2017 at approximately 2,393 geodetic stations including those in NOAA's National Continuously Operating Reference Station Network (NCN), plus many contained in the IGS-affiliated network. The adopted NCN velocity estimates may be obtained at NOAA (2021).
- A data set produced by National Aeronautics and Space Administration's (NASA's) Jet Propulsion Laboratory (JPL) that provides IGS14-consistent 3D velocities for more than 2,650 continuous GNSS stations distributed around the world. The latest results are available at NASA/JPL (2020).
- An unpublished data set produced in 2019 by Natural Resources Canada (NRCAN) for 3D velocities (some observed continuously and others in campaign mode) at geodetic stations located in and around Canada (M. Craymer, personal communication, 2019).

Three of the remaining six data sets are updated versions of the data sets used by Snay et al. (2018). They include the following:

- A data set produced by the University of Nevada Reno (UNR) (Blewitt et al. 2018) that provides estimated IGS14-consistent 3D velocities for more than 10,400 continuous GNSS stations distributed around the world. The latest UNR velocities are available at UNR (2021).
- A data set produced by Geodesy Advancing Geosciences and Earthscope (GAGE) which includes IGS14-consistent 3D velocities for more than 2,600 continuous GNSS stations distributed around the world, including those contained in University Navstar Consortium's (UNAVCO's) Plate Boundary Observatory (PBO) (Herring et al. 2016). The GAGE velocities are updated annually with the latest results available at UNAVCO (2021).
- A Making Earth System Data Records for Use in Research Environments (MEASUREs) data set that NASA's Jet Propulsion Laboratory and Scripps Orbit and Permanent Array Center jointly produce (Bock and Webb 2012). This data set provides

IGS08-consistent 3D velocities for more than 2,600 continuous GNSS stations distributed around the world. The MEASUREs velocities are updated weekly.

The three remaining data sets are the same as those used by Snay et al. (2016, 2018). They include the following:

- A data set published by McCaffrey et al. (2013) for GPS stations (some observed continuously and others in campaign mode) located in and around northwestern CONUS.
- The Southern California Earthquake Center data set known as Crustal Motion Model Four (Shen et al. 2011) for geodetic stations located mainly in and around southern California.
- An unpublished data set produced by the University of Alaska Fairbanks for 3D velocities at geodetic stations (some observed continuously, others in campaign mode) located in and around Alaska (J. Freymueller, personal communication, 2014).

While these latter three data sets do not directly contribute to determining IGS14-consistent 3D velocities at geodetic stations located in and around the Caribbean plate, they have been included to help transform the velocities of the 16 data sets from their adopted reference frames into the IGS14 reference frame, as discussed in the following paragraph.

Using the combination process described in Appendix A of Snay et al. (2016), the GNSS derived velocities from these 16 data sets were employed to estimate a single 3D IGS14 velocity for each of approximately 13,700 distinct geodetic stations. Of these stations, approximately 529 reside either within the chosen spherical rectangle for this paper or within approximately 100 km of this spherical rectangle. The remaining stations span the globe. Velocities at stations located around the world were included in the combination process to more accurately estimate the seven parameters required for each of the 16 data sets to transform its velocities from its associated reference frame to the IGS14 reference frame. Actually, a set of seven parameters is needed for each of only 15 of the data sets because the velocities of the IGS data set are already referred to IGS14. The seven parameters include three translation rates (\dot{T}_X , \dot{T}_Y , \dot{T}_Z), three rotation rates (\dot{R}_X , \dot{R}_Y , \dot{R}_Z), and a scale change rate (\dot{S}). Here the subscripts— X , Y , Z —pertain to the three axes of a traditional right-handed Earth-centered-Earth-fixed (ECEF) Cartesian coordinate system with the Z -axis approximating Earth's axis of rotation and the positive X -axis piercing Earth's equator near 0° longitude. See Snay et al. (2016) for additional information about the employed combination process.

In this paper, velocities contained in the 16 data sets are referred to as Stage-1 velocities; and the velocities estimates produced via the combination process are referred to as Stage-2 velocities. The diamonds appearing in Fig. 1 identify GNSS stations located in the spherical rectangle of this study. The color of each diamond corresponds to the station's Stage-2 vertical velocity. In subsequent sections of this paper, a two-step process is discussed which employs the Stage-2 velocities to estimate IGS14 velocities at the grid nodes of the specified spherical rectangle. The resulting velocities at these nodes are referred to as Stage-3 velocities. Stage-3 velocities correspond to the velocities encoded into the TRANS4D software.

The uncertainty assigned to a Stage-2 velocity component (east, north, up) of a geodetic station equals the minimum value of the reported uncertainties, pertaining to this velocity component, among all of the Stage-1 velocities at this station with the following restrictions: (1) the uncertainty of a Stage-2 horizontal velocity component cannot be smaller than 0.2 mm/year, and (2) the uncertainty of a Stage-2 vertical velocity component cannot be smaller than 0.3 mm/year. These lower bounds are consistent with the results presented in Fig. 2 of Saleh et al. (2021). The uncertainty of a Stage-2 velocity component was assigned in this way because

the various Stage-1 velocities for a station are based upon very similar sets of geodetic data and thus do not represent independent estimates. Also, it is not uncommon for different institutions to estimate different velocities with different uncertainties at a station even though they are using essentially the same data for that station. Thus, to be conservative, the uncertainty of each adopted Stage-2 velocity component involved in this study is assumed to equal one standard deviation.

Modeling Velocities

The employed velocity-modeling process is a two-step procedure that uses Stage-2 velocities to estimate Stage-3 velocities. Snay et al. (2018) discuss this process in some detail, thus only an outline is presented here. For the first step (called Step A), a preliminary model for the 3D velocity field is specified. This preliminary model may be imported from a previous study. Alternatively, this preliminary model may be developed by using equations to characterize velocities in terms of relevant parameters. For the second step (called Step B), a residual velocity is calculated for each available Stage-2 velocity located in the designated study area by subtracting from each Stage-2 velocity its corresponding velocity yielded by the preliminary model. Then the interpolation process, discussed in the following paragraph, is applied to the set of residual velocities to estimate an incremental velocity for each of several designated points located in the study area. For this study, these designated points will be the nodes of a two-dimensional grid spanning the previously specified spherical rectangle. Each of these incremental velocities are then added to its corresponding velocity, as generated via the preliminary model, to produce a Stage-3 velocity. Thus, via bilinear interpolation, the resulting set of Stage-3 velocities at the specified collection of grid nodes forms the foundation for an updated velocity model for all points located within the designated spherical rectangle.

In this paper, the spatial interpolation of the residual velocities is performed one component at a time (north, east, up) using all available residual velocities located within a “prespecified distance” of the location at which an estimated (residual) velocity is desired. The applied interpolation process is a variation of kriging (Goovaerts 1997). In particular, for each component of the residual velocities, a function needs to be estimated which relates the semi-variance between two available residual velocities to the distance between their respective locations. For each (residual) velocity component at a specified location, this function dictates how much each of the available residual velocities contributes to the estimated value of that component. For mathematical details, see Snay et al. (2018).

For this study, a prespecified distance of 100 km was used except when the resulting circular area around a given location contained less than seven residual velocities, in which case the prespecified distance was increased to 200 km unless there were no stations located within 200 km of the given location. In the latter case, then the new velocity at the location was set equal to its preliminary velocity. These exceptions were required to estimate velocities on isolated islands or at oceanic points located far from major land masses.

For this study, the employed preliminary model was such that IGS14 vertical velocities are equal to 0.0 mm/year at all locations, and the IGS14 horizontal velocities are equal to those defined by a rigid plate motion model for each of the seven tectonic plates/microplates residing, in whole or part, within the Caribbean study area as pictured in Fig. 1. This adopted set of plate motion models is discussed later in this paper. For now, however, it is somewhat

apparent that the estimated 3D velocity may be relatively crude because, for example, the tectonic plates are initially assumed to be fully rigid (and thus have essentially no vertical velocity), whereas each plate usually undergoes significant horizontal and vertical deformation near its boundaries with other plates. Thus, the process may need to be iterated. That is, the resulting Stage-3 estimates for the 3D velocities may need to serve as the preliminary velocities for a second solution in which the newer residual velocity should be smaller in magnitude than the original residual velocities. For this study, the estimation process was performed four times, with each successive solution relying on the results of its immediately previous solution.

Estimated Vertical Velocities

Fig. 2 presents a map of the resulting Stage-3 IGS14 vertical velocities found (after the fourth solution) within the larger land masses located in the adopted study area. Note that such velocities are not shown at places located more than 200 km from any geodetic station included in this study, and they are also not shown outside any land masses (even though TRANS4D may provide such velocity estimates via interpolation). Also, velocities are not shown at places where the standard deviations for these estimated velocities exceed 2.0 mm/year. The TRANS4D software, however, will output an IGS14 vertical velocity of 0.0 mm/year for those points located more than 200 km from any geodetic station used in this study, and this software will assign a nominal value of 2.2 mm/year for the standard deviation of this velocity. Note that TRANS4D may yield a nonzero vertical velocity when it transforms a zero-value IGS14 vertical velocity from IGS14 to its corresponding vertical velocity relative to a different reference frame (an inevitable consequence of frame transformations). Fig. 3 presents a map displaying standard deviations for the Stage-3 IGS14 vertical velocities located within the larger land masses.

Estimating Euler-Pole Parameters

Fig. 4 presents the collection of Stage-2 horizontal velocities relative to a horizontal reference frame defined by a newly determined Euler pole for a collection of stations located on the Caribbean plate. This Euler-pole reference frame minimizes horizontal velocities at selected locations on the Caribbean plate so as to emphasize where this plate is relatively stable and how other locations are moving relative to these locations. As such, the display of the horizontal velocity field relative to this Euler-pole-defined reference frame is more instructive than a display of the IGS14 horizontal velocity field.

The designation of Euler-pole parameters involves the determination of three parameters relative to some adopted reference frame. For this study, IGS14 serves as the adopted reference frame. Moreover, two of the three parameters correspond to the latitude φ and longitude λ at which a pole (that passes through the geocenter) pierces the Earth's surface and the third parameter is a rotation rate ω of the Earth's surface relative to this pole. Alternatively, a Euler pole can be quantified by designating three rotation rates; namely, a rotation rate about the X -axis (ω_X), another about the Y -axis (ω_Y), and another about the Z -axis (ω_Z), where (X , Y , Z) represent the three axes of an ECEF coordinate system with the X - and Y -axes located in the plane of the equator and with the Z -axis approximating Earth's axis of rotation. The two Euler-pole representations are related by the three equations

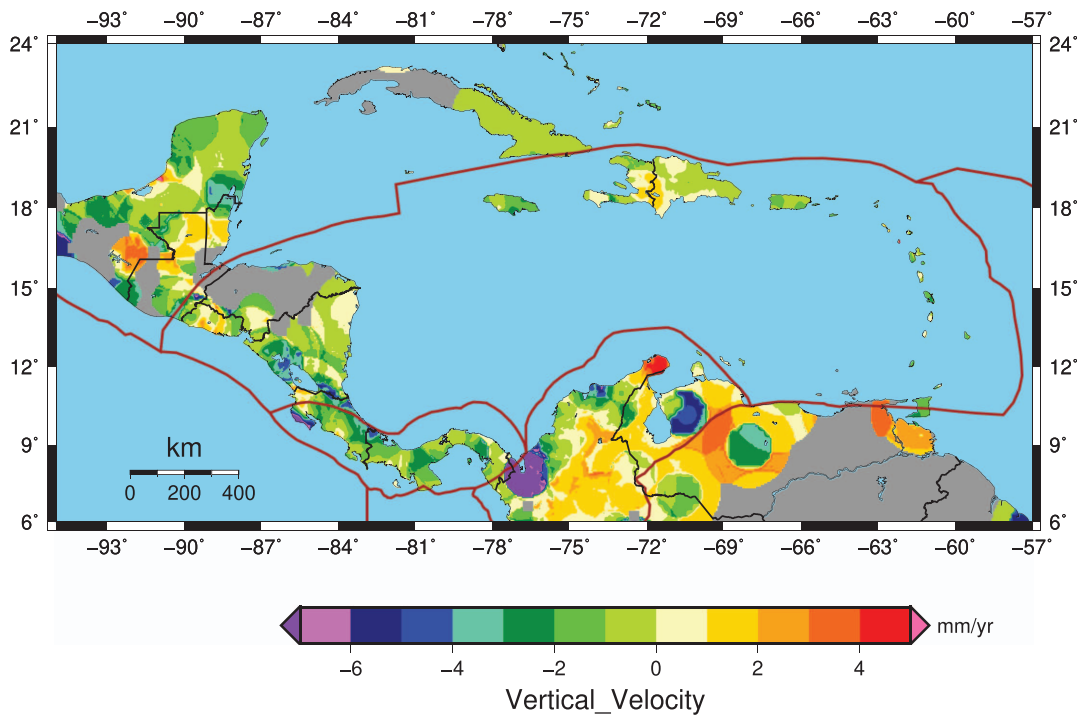


Fig. 2. (Color) Map of Stage-3 IGS14 vertical velocities at locations within the larger land masses. Gray areas identify locations where the standard deviations for these vertical velocities exceed 2.0 mm/year.

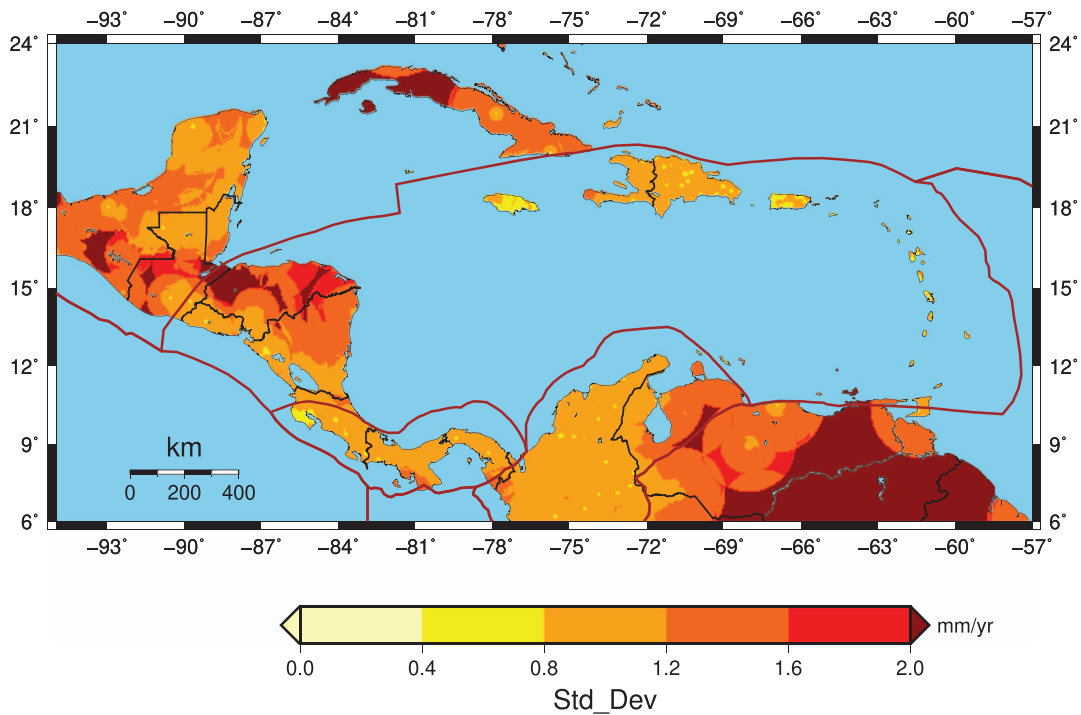


Fig. 3. (Color) Map of standard deviations for Stage-3 IGS14 vertical velocities at locations within the larger land masses.

$$\omega_X = \omega \cdot \cos \varphi \cdot \cos \lambda \quad (1)$$

$$\omega_Y = \omega \cdot \cos \varphi \cdot \sin \lambda$$

$$\omega_Z = \omega \cdot \sin \varphi$$

To obtain values for the three rotation rates (ω_X , ω_Y , ω_Z), the Stage-2 IGS14 horizontal velocities of the available 303 geodetic stations (that reside on the Caribbean plate) were employed in a weighted least-squares estimation process. This process yielded estimates for the three rotation rates which minimize the horizontal velocities that resulted by applying the estimated rotation rates to

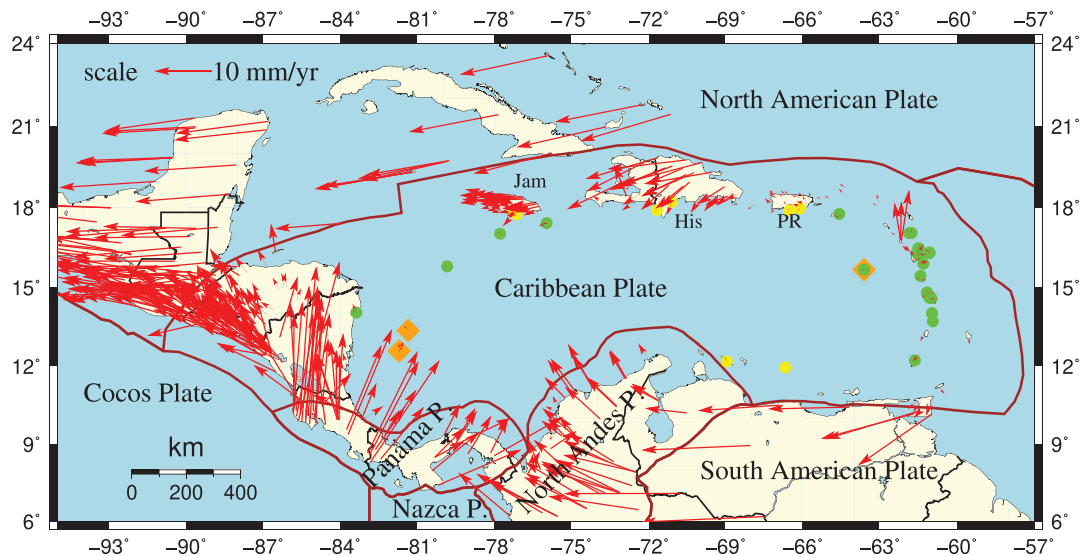


Fig. 4. (Color) Stage-2 horizontal velocities relative to the CATRF2014 reference frame. The green disks identify the 25 geodetic stations employed to estimate the Euler-pole parameters defining this reference frame. Yellow disks identify additional stations each of whose velocity is less than 1.0 mm/year relative to CATRF2014. Orange diamonds identify islands that may be located in the stable interior of the Caribbean plate. Jam = Jamaica; His = Hispaniola; and PR = Puerto Rico.

the weighted IGS14 velocities of selected stations. Note that the weight assigned to a Stage-2 horizontal velocity component was set to $1.0/\sigma^2$, where σ represents the estimated standard deviation of this velocity component.

More specifically, if (X_a, Y_a, Z_a) represent the IGS14 coordinates of a point, located on the Caribbean plate, whose estimated IGS14 velocity equals (V_{Xa}, V_{Ya}, V_{Za}) , and if rotation rates $(\omega_x, \omega_y, \omega_z)$ were applied to the IGS14 coordinates to produce a new reference frame, then the resulting velocities (V_{Xb}, V_{Yb}, V_{Zb}) that are relative to this new frame would be adequately approximated by the following:

$$V_{Xb} = V_{Xa} + (\omega_z) \cdot Y_a - (\omega_y) \cdot Z_a \quad (2)$$

$$V_{Yb} = V_{Ya} - (\omega_z) \cdot X_a + (\omega_x) \cdot Z_a$$

$$V_{Zb} = V_{Za} + (\omega_y) \cdot X_a - (\omega_x) \cdot Y_a$$

when ω_x , ω_y , and ω_z are each small in magnitude.

Thus, using least-squares estimation, one can estimate the values of ω_x , ω_y , and ω_z that best minimize the velocities (V_{Xb}, V_{Yb}, V_{Zb}) for some subset of geodetic stations residing on the Caribbean plate. As may be expected, when all 303 stations residing on this plate were involved, the resulting horizontal velocities at some of these stations were relatively large, especially those stations located near the periphery or unstable part of the Caribbean plate. Hence, the geodetic stations with larger resulting horizontal velocities were eliminated before performing a subsequent application of the estimation process to the remaining stations. This elimination procedure was iterated until all of the remaining stations had rotated horizontal velocities each of whose magnitude is smaller than 1.0 mm/year. Despite having such low velocities, several of the remaining stations reside within or near deforming tectonic blocks located within the Caribbean plate. These deforming blocks are identified in Fig. 8 of Smithe et al. (2015). Moreover, these blocks are located in the vicinity of Jamaica, Hispaniola, and/or Puerto Rico (see Fig. 4 to locate these three islands) or within 100 km of the South American coastline. Thus, for the sake of caution, the

geodetic stations residing on or near these deforming blocks were excluded when further estimating a set of Euler-pole parameters for the Caribbean plate relative to IGS14. In the end, only 25 of the 303 stations, residing on the Caribbean plate, were effectively involved in determining the desired Euler-pole parameters. These 25 stations are listed in Table 1, and they are displayed as green disks in Figs. 4 and 5. Note that all but four of these 25 stations reside in the eastern sector of the Caribbean plate. This distribution reflects a sampling problem in that the geodetic coverage of the Caribbean plate is poorly distributed because most of this plate resides under water. In addition, most of the 303 stations are located near the edge of the plate, where significant deformation occurs. The values of the three estimated rotation rates are

$$(\omega_x, \omega_y, \omega_z) = (-0.188, -4.730, 2.963) \text{ nrad/year} \quad (3)$$

whose respective standard deviations have the estimated values of (0.032, 0.066, 0.022) nrad/year. Note that nrad is short for nanoradian, that is, 10^{-9} radians.

These estimated rotation rates correspond to a counterclockwise rotation rate (ω) of 5.585 nrad/year about a pole that pierces Earth's surface at $\varphi = 32.04^\circ\text{N}$ and $\lambda = 92.78^\circ\text{W}$. It is important to emphasize that these Euler-pole parameters are relative to the IGS14 reference frame.

Estimated Horizontal Velocities

Fig. 4 presents the available Stage-2 horizontal velocities relative to the estimated Euler-pole parameters. Fig. 5 presents a map presenting the estimated Stage-3 horizontal velocities relative to these Euler-pole parameters. Fig. 6 presents the value of the larger of two standard deviations associated with Stage-3 horizontal velocities, that is, the standard deviation for the velocity's north-south component and that for its east-west component.

Table 1 shows that the transformation of IGS14 horizontal velocities to horizontal velocities relative to these Euler-pole parameters can involve changes on the order of 10 mm/year in

Table 1. Horizontal velocities at the 25 geodetic stations used to define the CATRF2014 reference frame plus horizontal velocities at eight additional stations

Site	Latitude (degrees north)	Longitude (degrees west)	IGS14		CATRF2014	
			north velocity (mm/year)	east velocity (mm/year)	north velocity (mm/year)	east velocity (mm/year)
ABD0	16.4743	61.4880	14.62 ± 0.92	10.49 ± 1.02	−0.83	−0.33
ABE1	16.4720	61.5090	16.02 ± 0.33	11.24 ± 0.32	0.58	0.42
ABMF	16.2623	61.5275	15.02 ± 0.20	10.76 ± 0.20	−0.23	−0.17
ADE0	16.2970	61.0860	16.02 ± 0.34	10.79 ± 0.36	0.39	−0.15
AVES	15.6670	63.6183	14.28 ± 1.30	10.65 ± 2.40	−0.19	−0.44
BGGY	17.0450	61.8610	15.81 ± 0.20	10.13 ± 0.20	0.53	−0.36
CAYS	15.7951	79.8461	6.30 ± 0.24	10.01 ± 0.49	−0.19	−0.20
CN01	17.0484	61.7654	15.93 ± 0.20	10.58 ± 0.24	0.61	0.09
CN04	14.0240	60.9740	15.54 ± 0.20	12.24 ± 0.20	−0.14	0.11
CN10	17.4152	75.9706	8.51 ± 0.20	8.64 ± 0.20	0.04	−0.78
CN11	17.0212	77.7841	7.89 ± 0.20	9.14 ± 0.20	0.34	−0.43
CN47	13.7108	60.9405	15.30 ± 0.20	12.50 ± 0.20	−0.40	0.21
CN48	15.4388	61.4216	14.80 ± 0.25	10.69 ± 0.29	−0.68	−0.67
CN49	15.6672	63.6183	14.11 ± 0.50	11.20 ± 0.38	−0.36	0.11
CRO1	17.7569	64.5843	13.53 ± 0.20	10.23 ± 0.20	−0.49	0.33
DESI	16.3040	61.0740	15.76 ± 0.42	10.93 ± 0.39	0.13	−0.01
DSD0	16.3120	61.0660	16.24 ± 0.70	10.15 ± 0.60	0.60	−0.78
FFT2	14.6015	61.0633	15.20 ± 1.09	12.48 ± 1.53	−0.44	0.66
FSDC	14.7350	61.1470	15.90 ± 0.49	12.07 ± 0.50	0.30	0.32
GOSI	16.2060	61.4810	15.90 ± 0.34	11.50 ± 0.34	0.45	0.54
GRE0	12.2218	61.6405	15.12 ± 0.20	13.19 ± 0.20	−0.26	0.18
LAM0	14.8130	61.1631	15.83 ± 0.32	11.56 ± 0.51	0.23	−0.15
LMMF	14.5948	60.9962	15.53 ± 0.20	12.48 ± 0.20	−0.14	0.65
MAG2	15.8900	61.3060	15.55 ± 0.33	11.82 ± 0.32	0.02	0.68
PUEC	14.0421	83.3820	5.17 ± 1.10	10.50 ± 2.00	0.54	−0.52
The following eight stations were not used in defining CATRF2014						
CN08	17.9034	71.6741	10.24 ± 0.20	9.00 ± 0.20	−0.38	−0.36
CN40	12.8004	68.9580	12.78 ± 0.20	12.30 ± 0.20	0.83	−0.36
CN42	11.9527	66.6823	12.93 ± 0.62	13.15 ± 1.70	−0.11	0.26
IGPR	17.9650	66.1070	12.88 ± 0.45	9.25 ± 0.55	−0.43	−0.43
KEMP	17.8618	77.2870	7.67 ± 0.50	9.32 ± 0.50	−0.14	0.22
MIPR	17.8862	66.5280	13.55 ± 0.20	9.31 ± 0.20	0.44	−0.38
TGDR	18.2080	71.0920	10.52 ± 0.65	8.45 ± 0.20	−0.39	−0.77
WARF	17.7486	77.1366	7.99 ± 0.30	8.24 ± 0.30	0.11	−0.94

Note: The latter eight stations were not used in defining CATRF2014 because they may reside in deforming areas of the Caribbean plate, even though the Stage-2 horizontal velocity of each has a magnitude less than 1.0 mm/year relative to CATRF2014.

both the north-south dimension and the east-west dimension. The magnitude of the velocity change at a point depends upon the distance between this point and the point where the Euler pole pierces Earth's surface and upon the magnitude of the rotation rate ω . Changes in vertical velocities, however, are small—approximately 0.1 mm/year in magnitude—which is generally below the accuracy with which vertical velocities can currently be measured using repeated GNSS observations. Nevertheless, vertical velocities will change because Euler pole rotations pertain to representing the Earth's surface as a sphere, whereas Earth's surface is better approximated as an ellipsoid of revolution.

As presented in Fig. 4, many of the 25 stations that are involved in determining these Euler-pole parameters reside on a north-south-trending chain of islands comprising part of the Lesser Antilles. However, near the northern extent of this island chain, a cluster of three stations is moving essentially northward at a rate of approximately 7 mm/year. These three stations reside near the Soufriere Hills Volcano located on the island of Montserrat.

Where is the Stable Interior of the Caribbean Plate?

According to the theory of plate tectonics, Earth's surface is covered, in large part, by a set of tectonic plates. Moreover, each

such plate is considered to be rigid unless some physical phenomena exert forces that cause all or part of this plate to deform. Such plate deformation is commonly found near plate boundaries because of frictional forces between adjacent plates. Even a plate's interior can deform due to some physical phenomena, such as glacial isostatic adjustment, but plate interiors are generally assumed to be rigid unless observed otherwise. If a particular plate has a rigid interior, there is a unique set of the Euler-pole parameters that will accurately characterize the motion of this interior relative to a specified spherical coordinate system that defines the location on Earth's surface (and slightly less accurately for an appropriate ellipsoidal reference system). In many cases, significant areas within a plate's interior are not rigid (i.e., are undergoing measurable deformation). In such cases it may be possible to find a set of Euler-pole parameters that greatly minimizes much of the horizontal motion over a considerable area of the given plate. In this paper, such a set of Euler-pole parameters was derived for the Caribbean plate. These parameters reveal that 21 geodetic stations located on islands residing in the eastern sector of the Caribbean plate, as well as four additional stations, are moving with sub-millimeter-per-year motion relative to the reference frame defined by these parameters. It may be that these Euler-pole parameters are not the Euler-pole parameters that define rigid motion for the "stable" interior of the Caribbean plate because many of these 21 stations are located

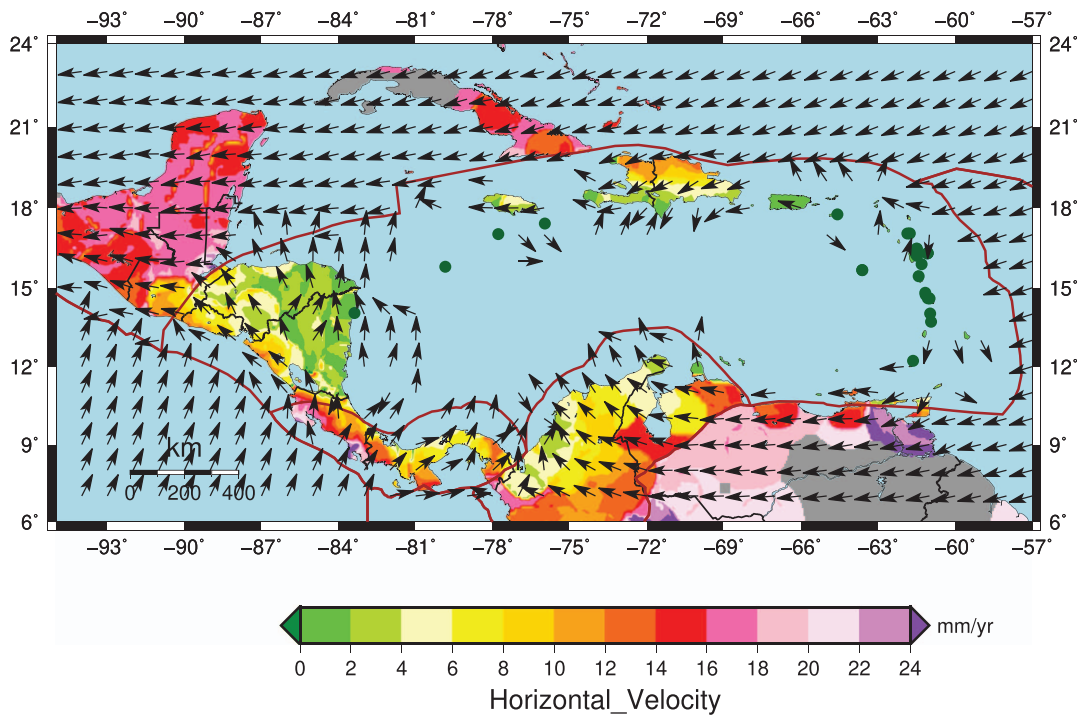


Fig. 5. (Color) Stage-3 horizontal velocities relative to CATRF2014 reference frame for the vicinity of the Caribbean plate. Colors (other than gray and blue) indicate speed, and arrows indicate direction when the corresponding speed exceeds 1.0 mm/year. The green disks identify the 25 geodetic stations employed to estimate the Euler-pole parameters defining this reference frame. Gray areas identify large land masses where standard deviations for the Stage-3 horizontal velocities exceed 2.0 mm/year in either the east-west or north-south dimension.

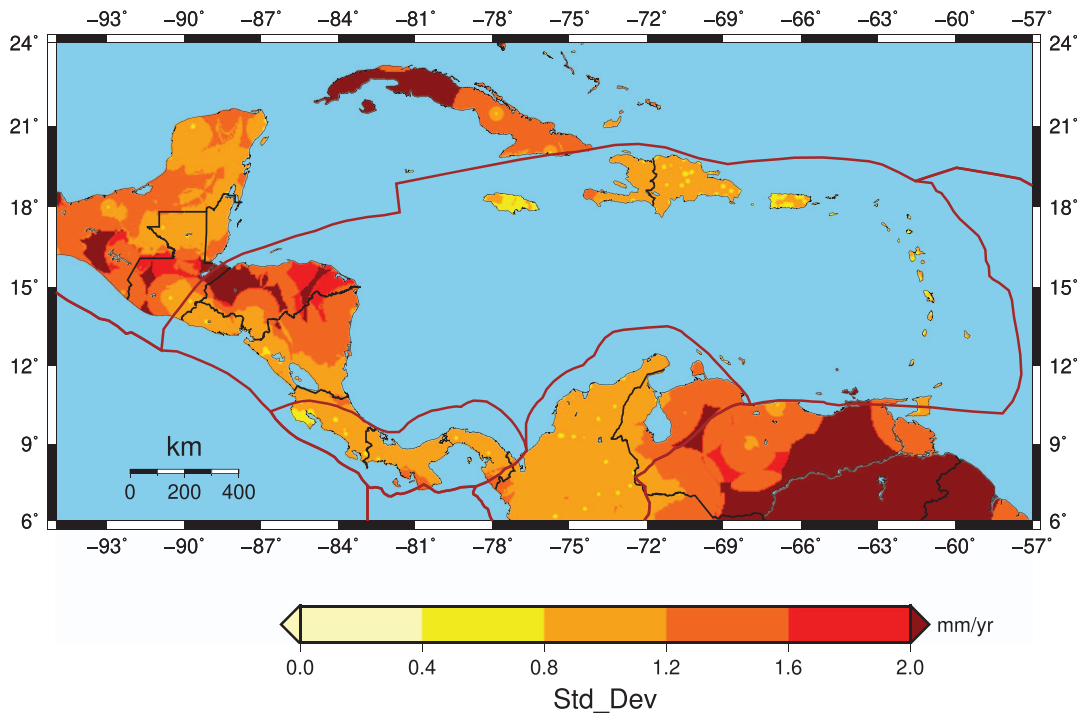


Fig. 6. (Color) Map showing the larger of the standard deviations for the north-south component and the standard deviations for the east-west component of the Stage-3 IGS14 horizontal velocities for locations within the large land masses of the study area.

approximately 300 km from the eastern boundary of the Caribbean plate, whereby some or all of these 21 stations may not be moving with respect to the stable interior of the Caribbean plate (if such stability exists).

Consequently, an anonymous reviewer of a previous version of this paper suggested that consideration be given to the geodetic stations located on three islands (namely, San Andres Island, Providencia Island, and Aves Ridge) that reside relatively closer to the

middle of the Caribbean plate than is the case for most of the 25 stations employed in this study. The orange diamonds displayed in Fig. 4 identify the location of these three islands, and Table 2 identifies six geodetic stations located on these three islands, together with their estimated IGS14 horizontal velocities. Note that two of these six stations (AVES and CN49, which are both located on Aves Ridge) were also used to estimate the Euler-pole parameters previously reported in this paper. The estimated Euler-pole parameters using only these six stations are

$$(\omega_x, \omega_y, \omega_z) = (-0.512, -4.014, 2.847) \text{ nrad/year} \quad (4)$$

and their respective standard deviations are (0.048, 0.241, 0.062) nrad/year.

As may have been expected, these estimated standard deviations are considerably larger than those previously obtained using the 25 stations listed in Table 1. Moreover, even though only six geodetic stations were employed, two of these stations exhibit horizontal velocities that have magnitudes exceeding 1.0 mm/year relative to this alternate reference frame for the Caribbean plate, as presented in Table 2. In particular, the magnitude of the estimated horizontal velocity at the station known as CN35 equals 1.22 mm/year relative to the reference frame associated with these alternative Euler-pole parameters.

With regard to the Euler-pole parameters presented in Eq. (3), NGS has a mission to promote spatial reference frames that serve the activities of geospatial professionals and others. Such reference frames need to be accurate and reliable. In particular, the definition of such frames should not vary over time. One way to accomplish this is to adopt one well-defined set of Euler-pole parameters that will remain relatively stable over time. It would be convenient, but not necessary, if these adopted parameters were also those that

adequately define the motion of a given tectonic plate's interior. Consequently, a Caribbean reference frame is being considered, which is defined in terms of a set of geodetic stations that move very little over time with respect to a derived set of Euler-pole parameters. Unfortunately, these Euler-pole parameters may not be the Euler-pole parameters that would characterize the motion of the rigid interior of the Caribbean plate. The Euler-pole parameters are poorly known at present, and they are likely to remain so for years to come, perhaps until scientists are able to determine accurate positional coordinates on the Caribbean seafloor.

Although the six geodetic stations listed in Table 2 are insufficient to accurately identify the stable interior of the Caribbean, the last column of Table 2 tabulates that each of these six stations moves less than 2 mm/year relative to the proposed CATRF2014 reference frame introduced in this paper.

Table 3 presents the adopted Euler-pole parameters for several tectonic plates relative to ITRF2014/IGS14. These parameters were employed to determine IGS14 horizontal velocities for points located on the seven tectonic plates involved in this paper when these points were located more than 200 km from any of the available geodetic stations. Then these computed IGS14 horizontal velocities were employed to determine CATRF2014 velocities for these distant locations in order to enable TRANS4D to provide a comprehensive horizontal velocity field for all points located in the spherical rectangle addressed in this paper.

Toward a New Caribbean Reference Frame

In or around 2025, NGS will modernize the National Spatial Reference System (NSRS) that provides coordinates for designated locations in the United States and its territories. NGS recently

Table 2. Horizontal velocities at the six geodetic stations used to define an alternate reference frame

Station/island	Latitude, (degrees north)	Longitude, (degrees west)	IGS14 north velocity (mm/year)	IGS14 east velocity (mm/year)	Alternate frame north/east velocities (mm/year)	CATRF2014 north/east velocities (mm/year)
AND5/San Andres	12.5863	81.2993	6.63 ± 1.30	11.90 ± 1.17	0.00/ - 0.44	0.88/ - 0.13
SAN0/San Andres	12.5805	81.7157	7.22 ± 0.20	12.78 ± 0.20	0.30/0.43	1.69/0.75
SANA/San Andres	12.5238	81.7294	6.57 ± 0.50	12.70 ± 0.60	-0.34/0.33	1.04/0.64
CN35/Providencia	13.3755	81.3630	6.73 ± 0.26	10.79 ± 0.39	-0.34/ - 1.17	1.02/ - 0.79
AVES/Aves Ridge	15.6670	63.9183	14.28 ± 1.30	10.65 ± 2.40	-0.02/ - 1.07	-0.19/ - 0.44
CN49/Aves Ridge	15.6672	63.6183	14.11 ± 0.50	11.20 ± 0.38	-0.19/ - 0.52	-0.36/0.11

Table 3. Plate rotation rates relative to ITRF2014/IGS14 as encoded into TRANS4D Version 0.3 (positive rotation rates are counterclockwise)

Plate	ω_x (nrad/year)	ω_y (nrad/year)	ω_z (nrad/year)	Source
North America	0.2668	-3.3677	-0.2956	Ding et al. (2019) ^a
Caribbean	-0.188	-4.730	2.963	This paper
Pacific	-1.983	5.076	-10.516	Altamimi et al. (2017)
Cocos	-10.380	-14.901	9.133	DeMets et al. (2010) ^b
South America	-1.309	-1.459	-0.679	Altamimi et al. (2017)
Nazca	-1.614	-7.486	7.869	Altamimi et al. (2017)
Panama	2.088	-23.037	6.729	Kreemer et al. (2014) ^b
North Andes	-1.964	-1.518	0.400	Mora-Páez et al. (2019) ^c

^aDing et al. (2019) provides both rotation rates and translation rates for describing the motion of the stable North American plate relative to ITRF2008/IGS08 as specified in their Table 2 for their ITRF-GEO-ICE6G model after outlier detection. For this study, only their rotation rates (and not their translation rates) were used to approximate the North American plate's motion relative to ITRF2014/IGS14.

^bDeMets et al. (2010) and Kreemer et al. (2014) provide rotation rates for the Cocos and Panama plates, respectively, relative to the Pacific plate. Those rates were converted to rates relative to ITRF2014/IGS14 by using rates for the Pacific plate relative to ITRF2014/IGS14 as published by Altamimi et al. (2017).

^cMora-Páez et al. (2019) provides rotation rates for the North Andes plate relative to the South American plate. Those rates were converted to rates relative to ITRF2014/IGS14 by using the rates for the South American plate relative to ITRF2014/IGS14 as published by Altamimi et al. (2017).

published a report (NGS 2021) that addresses the geometric aspects of the forthcoming NSRS modernization. The NSRS currently includes three geometric reference frames (historically called “horizontal datums”) which are known as NAD 83(2011), NAD 83(PA11), and NAD 83(MA11), referenced to the North America, Pacific, and Mariana tectonic plates, respectively. These reference frames are used to define the geodetic latitudes, geodetic longitudes, and ellipsoid heights for points located in the US and its territories. These three frames will be replaced with four new reference frames, to be called

- North American Terrestrial Reference Frame of 2022 (NATRF2022).
- Pacific Terrestrial Reference Frame of 2022 (PATRF2022).
- Caribbean Terrestrial Reference Frame of 2022 (CATRF2022).
- Mariana Terrestrial Reference Frame of 2022 (MATRF2022).

According to NGS (2021, p. vii), “The time-dependent Cartesian coordinates of any point on Earth in any of these four plate-fixed frames will be defined relative to the time-dependent Cartesian coordinates in ITRF2020. The relative relationship will rely on a plate rotation model for each tectonic plate associated with each frame. This relationship will rely on rotations about the three ITRF axes (called Euler-pole parameters). . . . Such time-dependent coordinates will exhibit coordinate stability in areas of the continent where motion of the tectonic plate is fully characterized by plate rotation. All remaining velocities (including horizontal motions induced directly or indirectly by adjoining tectonic plates, horizontal motions induced by glacial isostatic adjustment, other horizontal motions, and all vertical motions in their entirety) will be captured by a model, tentatively called an Intra-Frame Velocity Model (IFVM).”

NGS would prefer that the three “time-dependent rotations” for a particular plate would equate to the three rotation rates characterizing *the* Euler-pole parameters for that plate. However, NGS (2021, p. 17) acknowledges that the Euler-pole parameters for the Caribbean plate were rather uncertain at the time that this paper was written. Thankfully, the availability of additional geodetic data since then provides an effective alternative to *the* Euler-pole parameters of the Caribbean plate, as addressed in this paper. If NGS were to adopt the Euler-pole parameters presented in this paper, then Fig. 2 illustrates the estimated vertical velocities that would be associated with the IFVM for CATRF2022 and Fig. 5 illustrates the estimated horizontal velocities that would be associated with this IFVM. However, more accurate estimates for the Euler-pole parameters of the Caribbean plate and for its associated IFVM velocities may become available before the CATRF2022 is adopted. Thus, the velocities relative to the Euler-pole parameters, given in this paper, will be identified as belonging to the CATRF2014 reference frame. Mathematical details for transforming IGS14 positional coordinates to CATRF2014 positional coordinates are presented in the Appendix of this paper.

Puerto Rico and the US Virgin Islands

In addition to providing a reference frame for the United States, NGS is responsible for providing official reference frames for US territories. In the vicinity of the Caribbean plate, these territories include Puerto Rico and the US Virgin Islands. Fig. 7 presents a map of the area around these two territories and the horizontal velocity field that would result if NGS were to adopt the values

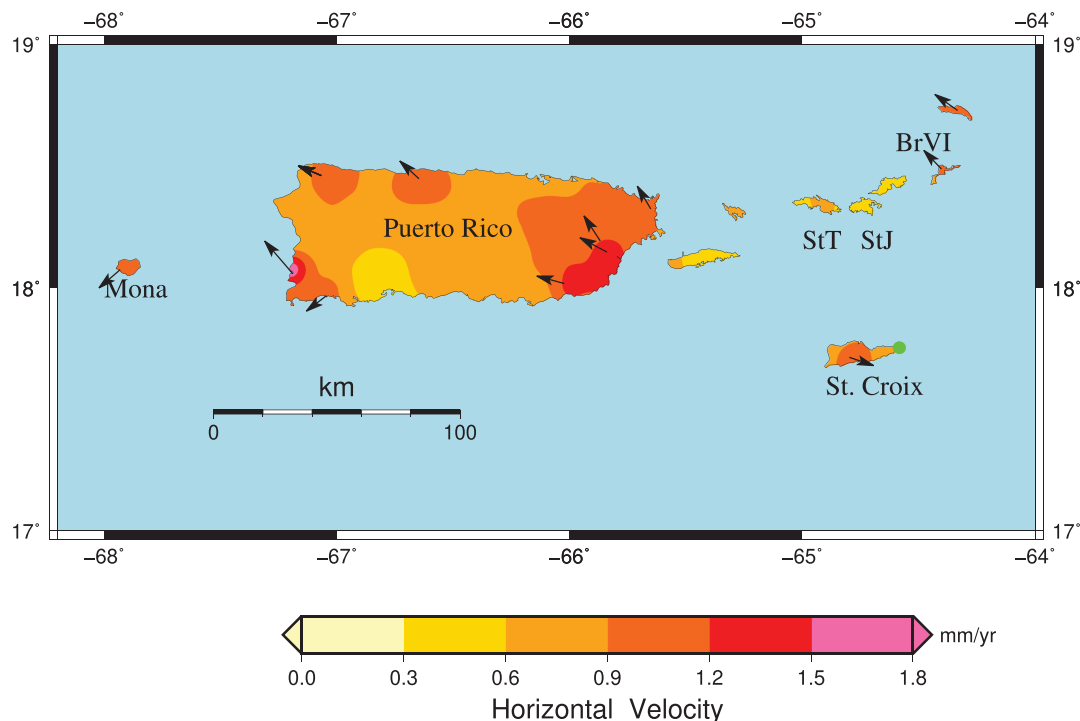


Fig. 7. (Color) Map of Stage-3 horizontal velocities relative to the CATRF2014 reference frame in the vicinity of Puerto Rico and the US Virgin Islands. Vectors represent horizontal velocities at those geodetic stations where such velocities have magnitudes exceeding 1.0 mm/year. The green disk identifies a geodetic station (called CROI) involved in estimating Euler-pole parameters for the Caribbean plate. StT = Saint Thomas; StJ = St. John; and BrVI = British Virgin Islands.

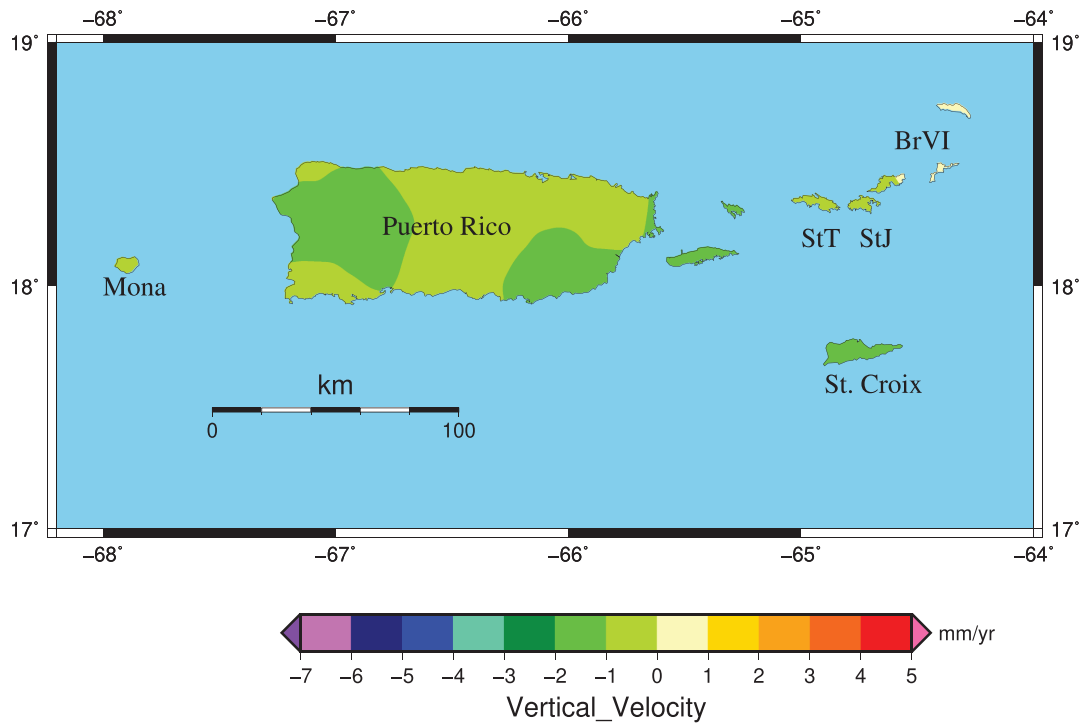


Fig. 8. (Color) Map of Stage-3 CATRF2014 vertical velocities in the vicinity of Puerto Rico and the US Virgin Islands. StT = St. Thomas; StJ = St. John; and BrVI = British Virgin Islands.

of the Caribbean Euler-pole parameters estimated herein. Note that Puerto Rico includes the largest island shown in Fig. 7 plus the two smaller islands located to the immediate east of this largest island. Also note that the US Virgin Islands include St. Thomas, St. John, and Saint Croix as identified in Fig. 7. The remaining islands located in the northeastern corner of Fig. 7 are part of the British Virgin Islands, and the island to the west of Puerto Rico is called Mona.

Tectonophysicists generally agree that the islands of Puerto Rico, Saint Thomas, and Saint John reside on a microplate that moves relative to the interior of the Caribbean plate (Byrne et al. 1985; Masson and Scanlon 1991; Jansma et al. 2000; Jansma and Mattioli 2005; Benford et al. 2012; Liu and Wang 2015; Symithe et al. 2015). Hence, in this study, only one geodetic station located within the area depicted in Fig. 7 was employed to estimate values for the CATRF2014 Euler-pole parameters (namely, station CROI located near the extreme eastern extent of St. Croix). As a result, locations in Puerto Rico move essentially westward at speeds between 0.3 and 1.8 mm/year, and locations in the US Virgin Islands move horizontally at speeds between 0.3 and 1.2 mm/year relative to CATRF2014. Furthermore, Fig. 8 presents a map of Stage-3 IGS14 vertical velocities for the same area. These velocities correspond to rates ranging between -2.0 and 0.0 mm/year (where negative rates correspond to subsidence). It is also expected that any newer IGS reference frame adopted within the next few years should provide velocities that differ only insignificantly from the current IGS14 velocities (except in such cases as the occurrence of a nearby earthquake).

Summary

This paper introduces Version 0.3 of the TRANS4D software. This version provides a 3D velocity model for a neighborhood of the

Caribbean plate in the form of a 2D grid (in latitude and longitude) which has a mesh of 0.0625° by 0.0625° . While the 3D velocities stored in TRANS4D are referred to the IGS14 reference frame, this software is capable of transforming them to several other popular reference frames, plus to the newly introduced reference frame, called CATRF2014. The transformation from IGS14 to this latter reference frame is defined in terms of three Euler-pole parameters that minimize the horizontal motion of 25 geodetic stations in such a way that each of these 25 stations has a horizontal velocity whose Stage-2 magnitude is less than 1.0 mm/year relative to CATRF2014.

Appendix. Transforming Positional Coordinates

Within the context of TRANS4D, positional coordinates for a location are assumed to vary with respect to time. Thus, when specifying positional coordinates, it is necessary to also specify the time to which they refer. Let $X(t)_a$, $Y(t)_a$, and $Z(t)_a$ denote the positional coordinates of a location at time t referred to reference frame a in a 3D ECEF Cartesian coordinate system. Similarly, let $X(t)_b$, $Y(t)_b$, and $Z(t)_b$ denote the positional coordinates of this same location at time t referred to reference frame b also in a 3D ECEF Cartesian coordinate system. Within TRANS4D, the coordinates in frame a are approximately related to those in frame b (both at time t) via the following equations of a 14-parameter transformation:

$$X(t)_b = T_x(t) + [1 + S(t)]X(t)_a + R_z(t)Y(t)_a - R_y(t)Z(t)_a$$

$$Y(t)_b = T_y(t) - R_z(t)X(t)_a + [1 + S(t)]Y(t)_a + R_x(t)Z(t)_a$$

$$Z(t)_b = T_z(t) + R_y(t)X(t)_a - R_x(t)Y(t)_a + [1 + S(t)]Z(t)_a \quad (5)$$

Here X , Y , and Z represent rectilinear coordinates expressed in meters, and t represents time expressed in years. Furthermore, $T_x(t)$, $T_y(t)$, and $T_z(t)$ are translations along the x -, y -, and z -axis, respectively, each expressed in meters; and $R_x(t)$, $R_y(t)$, and $R_z(t)$ are counterclockwise rotations about these same three axes, each expressed in radians; and $S(t)$ is a unitless quantity representing the differential scale between reference frame a and reference frame b . These approximate equations suffice because the three rotations have relatively small magnitudes. Note that each of the seven quantities is represented as a function of time because modern geodetic technology has enabled scientists to detect their time-related variations with some degree of accuracy. In TRANS4D, these time-related variations are assumed to be linear, so that

$$T_X(t) = T_X(t_0) + \dot{T}_X \cdot (t - t_0) \quad (6)$$

$$T_Y(t) = T_Y(t_0) + \dot{T}_Y \cdot (t - t_0)$$

$$T_Z(t) = T_Z(t_0) + \dot{T}_Z \cdot (t - t_0)$$

$$S(t) = S(t_0) + \dot{S} \cdot (t - t_0)$$

$$R_X(t) = R_X(t_0) + \dot{R}_X \cdot (t - t_0)$$

$$R_Y(t) = R_Y(t_0) + \dot{R}_Y \cdot (t - t_0)$$

$$R_Z(t) = R_Z(t_0) + \dot{R}_Z \cdot (t - t_0)$$

where t_0 denotes a prespecified time of reference (expressed in years). Also, the seven quantities of the form $P(t_0)$ plus the seven quantities of the form \dot{P} are constants. Note that a dot over a variable represents the rate of the corresponding variable with respect to time (in years). Thus, the seven equations of Eq. (6) give rise to 14 parameters, but note that the values of seven of these parameters depend on the value chosen for t_0 .

In the special case of a transformation from IGS14 coordinates to CATRF2014 coordinates

$$\dot{T}_X = \dot{T}_Y = \dot{T}_Z = \dot{S} = 0$$

$$\begin{aligned} (\dot{R}_X, \dot{R}_Y, \dot{R}_Z) &= (\omega_X, \omega_Y, \omega_Z) \\ &= (-0.188, -4.730, 2.963) \text{ nrad/year} \end{aligned} \quad (7)$$

Furthermore, if t_0 is set equal to 2010.00, which is the adopted reference epoch of the currently published IGS14 coordinates, then

$$\begin{aligned} T_X(t_0) &= T_Y(t_0) = T_Z(t_0) = S(t_0) = R_X(t_0) = R_Y(t_0) \\ &= R_Z(t_0) = 0 \end{aligned} \quad (8)$$

and Eq. (5) becomes

$$\begin{aligned} X(t)_b &= X(t)_a + [\omega_Z \cdot Y(t)_a - \omega_Y \cdot Z(t)_a] \cdot (t - 2010.00) \\ Y(t)_b &= Y(t)_a + [\omega_X \cdot Z(t)_a - \omega_Z \cdot X(t)_a] \cdot (t - 2010.00) \\ Z(t)_b &= Z(t)_a + [\omega_Y \cdot X(t)_a - \omega_X \cdot Y(t)_a] \cdot (t - 2010.00) \end{aligned} \quad (9)$$

where the subscript a identifies IGS14 coordinates, and the subscript b identifies CATRF2014 coordinates, both referred to an arbitrary time, denoted as t .

From Eq. (9), it follows that to compute a location's coordinates at time t relative to the CATRF2014 reference frame, then the IGS14 coordinates for this location at time t needs to be determinable. This may be done by knowing the location's IGS14 positional

coordinates at some arbitrary time together with knowing this location's IGS14 velocity.

Also, from Eq. (9), it follows that the CATRF2014 positional coordinates for a location equal the location's IGS14 positional coordinates when $t = 2010.00$.

Data Availability Statement

The TRANS4D (Version 0.3) software is written in FORTRAN-90. This software, together with its associated data files and user's guide, may be obtained by contacting the corresponding author.

Acknowledgments

The authors thank the many people and institutions that were involved in collecting and/or processing the geodetic data included in this study. The authors also thank Daniel Gillins and two anonymous reviewers for suggestions that improved the presentation of this paper. This paper was supported, in part, by the National Geodetic Survey. The figures have been drawn using Generic Mapping Tools (Wessel and Smith 1998).

References

- Altamimi, Z., L. Metivier, P. Rebischung, H. Rouby, and X. Collilieux. 2017. "ITRF2014 plate motion model." *Geophys. J. Int.* 209 (3): 1906–1912. <https://doi.org/10.1093/gji/ggx136>.
- Altamimi, Z., P. Rebischung, L. Metivier, and X. Collilieux. 2016. "ITRF2014: A new release of the International Terrestrial Reference Frame modeling non-linear station motions." *J. Geophys. Res. Solid Earth* 121 (8): 6109–6131. <https://doi.org/10.1002/2016JB013098>.
- Benford, B., C. DeMets, B. Tikoff, P. Williams, L. Brown, and M. Wiggins-Grandison. 2012. "Seismic hazard along the southern boundary of the Gônave microplate: Block modelling of GPS velocities from Jamaica and nearby islands, northern Caribbean." *Geophys. J. Int.* 190 (1): 59–74. <https://doi.org/10.1111/j.1365-246X.2012.05493.x>.
- Bird, P. 2003. "An updated digital model of plate boundaries." *Geochem. Geophys. Geosyst.* 4 (3): 1027. <https://doi.org/10.1029/2001GC000252>.
- Blewitt, G., W. C. Hammond, and C. Kreemer. 2018. "Harnessing the GPS data explosion for interdisciplinary science." *Eos*. Accessed September 24, 2018. <https://doi.org/10.1029/2018EO104623>.
- Bock, Y., and F. Webb. 2012. "MEaSURES solid earth science ESDR system." Accessed January 21, 2019. http://sopac-ftp.ucsd.edu/pub/timeseries/measures/timeseriesModelTermsSummary.MEASURES_Combination_20130627.txt.
- Byrne, D. B., G. Suarez, and W. R. McCann. 1985. "Muertos trough subduction—Microplate tectonics in the northern Caribbean?" *Nature* 317 (6036): 420–421. <https://doi.org/10.1038/317420a0>.
- DeMets, C., R. G. Gordon, and D. F. Argus. 2010. "Geologically current plate motions." *Geophys. J. Int.* 181 (1): 1–80. <https://doi.org/10.1111/j.1365-246X.2009.04491.x>.
- Ding, K., J. T. Freymueller, P. He, Q. Wang, and C. Xu. 2019. "Glacial isostatic adjustment, intraplate strain, and relative sea level changes in Eastern United States." *J. Geophys. Res. Solid Earth* 124 (6): 6056–6071. <https://doi.org/10.1029/2018JB017060>.
- Ellis, A., et al. 2018. "GPS constrains on deformation in northern Central America from 1999 to 2017. Part 1: Time-dependent modelling of large regional earthquakes and their post-seismic effects." *Geophys. J. Int.* 214 (3): 2177–2194. <https://doi.org/10.1093/gji/ggy249>.
- Ellis, A., et al. 2019. "GPS constraints on deformation in northern Central America from 1999 to 2017, Part 2: Block rotations and fault slip rates, fault locking and distributed deformation." *Geophys. J. Int.* 218 (2): 729–754. <https://doi.org/10.1093/gji/ggz173>.
- Goovaerts, P. 1997. *Geostatistics for natural resources evaluation*. Oxford, UK: Oxford University Press.

- Herring, T. A., T. I. Melbourne, M. H. Murray, M. A. Floyd, W. M. Szeliga, R. W. King, D. A. Phillips, C. M. Puskas, M. Santillan, and L. Wang. 2016. "Plate Boundary Observatory and related networks: GPS data analysis methods and geodetic products." *Rev. Geophys.* 54 (4): 759–808. <https://doi.org/10.1002/2016RG000529>.
- Jansma, P. E., and G. S. Mattioli. 2005. "GPS results from Puerto Rico and the Virgin Islands: Constraints on tectonic setting and rates of active faulting." In Vol. 385 of *GSA Special Papers Series: Active Tectonics and Seismic Hazards of Puerto Rico, the Virgin Islands, and Offshore Areas*, edited by P. Mann, 13–30. Boulder, CO: Geological Society of America. <https://doi.org/10.1130/SPE385>.
- Jansma, P. E., G. S. Mattioli, A. Lopez, C. DeMets, T. H. Dixon, P. Mann, and E. Calais. 2000. "Neotectonics of Puerto Rico and the Virgin Islands, northeastern Caribbean, from GPS geodesy." *Tectonics* 19 (6): 1021–1037. <https://doi.org/10.1029/1999TC001170>.
- Kreemer, C., G. Blewitt, and E. C. Klein. 2014. "A geodetic plate motion and global strain rate model." *Geochem. Geophys. Geosyst.* 15 (10): 3849–3889. <https://doi.org/10.1002/2014GC005407>.
- Liu, H., and G. Wang. 2015. "Relative motion between St. Croix and the Puerto Rico–Northern Virgin Islands block derived from continuous GPS observations (1995–2014)." *Int. J. Geophys.* 2015: 915753. <https://doi.org/10.1155/2015/915753>.
- Masson, D. G., and K. M. Scanlon. 1991. "The neotectonic setting of Puerto Rico." *Geol. Soc. Am. Bull.* 103 (1): 144–154. [https://doi.org/10.1130/0016-7606\(1991\)103<0144:TNSOPR>2.3.CO;2](https://doi.org/10.1130/0016-7606(1991)103<0144:TNSOPR>2.3.CO;2).
- McCaffrey, R., R. W. King, S. J. Payne, and M. Lancaster. 2013. "Active tectonics of northwestern U.S. inferred from GPS-derived surface velocities." *J. Geophys. Res. Solid Earth* 118 (2): 709–723. <https://doi.org/10.1029/2012JB009473>.
- Mora-Páez, H., et al. 2019. "Crustal deformation in the northern Andes—A new GPS velocity field." *J. South Am. Earth Sci.* 89 (Jan): 76–91. <https://doi.org/10.1016/j.jsames.2018.11.002>.
- Moritz, H. 2000. "Geodetic Reference System 1980." *J. Geod.* 74 (1): 128–133. <https://doi.org/10.1007/s001900050278>.
- NASA/GSFC (National Aeronautics and Space Administration/Goddard Space Flight Center). 2019. "IGS20P45_all.ssc.Z." *CDDIS: NASA's Archive of Space Geodesy Data*. Accessed July 28, 2021. <https://cddis.nasa.gov/archive/gnss/products/2130/>.
- NASA/JPL (National Aeronautics and Space Administration/Jet Propulsion Laboratory). 2020. "GNSS science data: Table 2." *Jet Propulsion Laboratory at the California Institute of Technology*. Accessed July 28, 2021. <https://sideshow.jpl.nasa.gov/post/tables/table2.html>.
- NGS (National Geodetic Survey). 2020. "Delayed release of the modernized NSRS." Accessed April 14, 2021. <https://geodesy.noaa.gov/datum/newdatums/NSRSModernizationNewsIssue20.pdf>.
- NGS (National Geodetic Survey). 2021. "Blueprint for the modernized NSRS, Part 1: Geometric coordinates and terrestrial reference frames." Accessed June 2, 2021. https://geodesy.noaa.gov/library/pdfs/NOAA_TR_NOS_NGS_0062.pdf.
- NOAA (National Oceanic and Atmospheric Administration). 2021. "Table of ITRF2014 GNSS coordinates." *National Geodetic Survey*. Accessed July 28, 2021. https://noaa-cors-pds.s3.amazonaws.com/coord/coord_14/itrf2014_geo.comp.txt.
- Rebischung, P., Z. Altamimi, J. Ray, and B. Garayt. 2016. "The IGS contribution to ITRF2014." *J. Geod.* 90 (7): 611–630. <https://doi.org/10.1007/s00190-016-0897-6>.
- Saleh, J., S. Yoon, K. Choi, L. Sun, R. Snay, P. McFarland, S. Williams, D. Haw, and F. Coloma. 2021. "1996–2017 GPS position time series, velocities and quality measures for the CORS network." *J. Appl. Geodesy* 15 (2): 105–115. <https://doi.org/10.1515/jag-2020-0041>.
- Sánchez, L., and H. Drewes. 2020. "Geodetic monitoring of variable surface deformation in Latin America." In Vol. 152 of *Proc., Int. Association of Geodesy Symposia Series*, 1–12. Berlin, Heidelberg: Springer. https://doi.org/10.1007/1345_2020_91.
- Shen, Z. K., R. W. King, D. C. Agnew, M. Wang, T. A. Herring, D. Dong, and P. Fang. 2011. "A unified analysis of crustal motion in Southern California, 1970–2004: The SCEC crustal motion map." *J. Geophys. Res. Solid Earth* 116 (11): B11402. <https://doi.org/10.1029/2011JB008549>.
- Snay, R. A., J. T. Freymueller, M. R. Craymer, C. F. Pearson, and J. Saleh. 2016. "Modeling 3-D crustal velocities in the United States and Canada." *J. Geophys. Res. Solid Earth* 121 (7): 5365–5388. <https://doi.org/10.1002/2016JB012884>.
- Snay, R. A., J. Saleh, and C. F. Pearson. 2018. "Improving TRANS4D's model for vertical crustal velocities in Western CONUS." *J. Appl. Geodesy* 12 (3): 209–227. <https://doi.org/10.1515/jag-2018-0010>.
- Symithe, S., E. Calais, J. B. de Chabaliere, R. Robertson, and M. Higgins. 2015. "Current block motions and strain accumulation on active faults in the Caribbean." *J. Geophys. Res. Solid Earth* 120 (5): 3748–3774. <https://doi.org/10.1002/2014JB011779>.
- UNAVCO (University Navstar Consortium). 2021. "GPS/GNSS data." *Plate Boundary Observatory*. Accessed July 28, 2021. https://data.unavco.org/archive/gnss/products/velocity/cwu.final_igs14.vel.
- UNR (University of Nevada Reno). 2021. "Website of Nevada Geodetic Laboratory." Accessed July 28, 2021. <http://geodesy.unr.edu>.
- Wang, G., H. Liu, G. S. Mattioli, M. M. Miller, K. Feaux, and J. Braun. 2019. "CARIB18: A stable geodetic reference frame for geological hazard monitoring in the Caribbean region." *Remote Sensing* 11 (6): 680. <https://doi.org/10.3390/rs11060680>.
- Wessel, P., and W. H. F. Smith. 1998. "New, improved version of generic mapping tools released." *EOS Trans. Am. Geophys. Union* 79 (47): 579. <https://doi.org/10.1029/98EO00426>.